

*Utilization of agro-waste for removal
of toxic hexavalent chromium: surface
interaction and mass transfer studies*

**R. P. Mokkapati, V. N. Ratnakaram &
J. S. Mokkapati**

**International Journal of
Environmental Science and
Technology**

ISSN 1735-1472

Int. J. Environ. Sci. Technol.
DOI 10.1007/s13762-017-1443-7



Your article is protected by copyright and all rights are held exclusively by Islamic Azad University (IAU). This e-offprint is for personal use only and shall not be self-archived in electronic repositories. If you wish to self-archive your article, please use the accepted manuscript version for posting on your own website. You may further deposit the accepted manuscript version in any repository, provided it is only made publicly available 12 months after official publication or later and provided acknowledgement is given to the original source of publication and a link is inserted to the published article on Springer's website. The link must be accompanied by the following text: "The final publication is available at link.springer.com".

Utilization of agro-waste for removal of toxic hexavalent chromium: surface interaction and mass transfer studies

 R. P. Mokkapati¹ · V. N. Ratnakaram² · J. S. Mokkapati³

 Received: 20 February 2016/Revised: 19 May 2017/Accepted: 15 July 2017
 © Islamic Azad University (IAU) 2017

Abstract Abundantly available agricultural waste materials (banana bunch, sorghum stem and casuarinas fruit) are processed with negligible cost and are found to be highly suitable as biosorbents for chromium(VI) removal from aqueous environment due to high surface area and functional groups of adsorbents. The equilibrium data have been analyzed for the adsorbate–adsorbate/adsorbent interactions and found to be fitted to the data in the order, Hill–de Boer \geq Fowler–Guggenheim \cong Frumkin $>$ Kiselev. To determine the characteristic parameters for process design, mass transfer studies have been carried out using two-parameter isotherm models (Harkins–Jura, Halsey, Smith, El-Awady and Flory–Huggins) and three-parameter isotherm models (Redlich–Peterson and Sips) which are applied to the experimental data. The fitness of the isotherms describes that both mono- and multilayer adsorptions occur in the present studied three biosorbents in preference to the latter. The mechanism of adsorption has been studied using diffusion kinetic models (viz. liquid film diffusion, Dunwald–Wagner intra-particle diffusion model

and moving boundary model) and described the possibility of diffusion in the order of banana bunch–stem powder $>$ sorghum stem powder $>$ casuarinas fruit powder in terms of diffusion coefficients. In essence of all the results, the selected adsorbents can be used as a potential adsorbent for the removal of Cr(VI) from aqueous solutions.

Keywords Agricultural waste · Biosorption · Chromium(VI) removal · Diffusion · Mass transfer · Surface interaction

Introduction

Disposal of agricultural wastes adversely affects the quality of air, water and soil, leading to many problems including unbalanced natural ecological systems and increase in eutrophication (Sharma et al. 2010). About 500 Mt of crop residues is generated every year as per the estimation of the Ministry of New and Renewable Energy (MNRE 2009), Government of India. In spite of the traditional uses of crop residues (such as fuel, roof thatching, animal feed, fodder, composting and packaging), about 91–141 Mt of crop residues per year is estimated as surplus in India (IARI 2012). The surplus residues are burnt which is one of the noteworthy sources of atmospheric aerosols, carbon dioxide (CO₂), carbon monoxide (CO), methane (CH₄), volatile organic compounds (VOC), nitrogen oxides and halogen compounds (Guyon et al. 2005), which exhibit impact on climate as well as human health (van der Werf et al. 2006; Irwin 2014). Effect on climate includes the formation of dense ‘brown clouds’ in South Asia (Gustafsson et al. 2009) and smoke particles impact by serving as cloud-condensation nuclei (CCN) and changing the cloud microphysical and optical properties (Cattani et al. 2006).

Editorial responsibility: H.N. Hsieh.

Electronic supplementary material The online version of this article (doi:10.1007/s13762-017-1443-7) contains supplementary material, which is available to authorized users.

✉ V. N. Ratnakaram
doctornadh@yahoo.co.in

¹ Department of Chemistry, ANUCET, Acharya Nagarjuna University, Guntur 522510, India

² GITAM University, Bengaluru, Karnataka 561203, India

³ Institute of Environmental Sciences, Jagiellonian University, Kraków 30-387, Poland

The common aquatic pollutant in its hexavalent state Cr(VI) released by industrial activities into natural waters has detrimental effects on both the living organisms and the ecosystems (Igwe and Abia 2003; Rana et al. 2004). It has very adverse effects, and strong exposure causes skin irritation, lung cancer, kidney, liver and gastric damage, epigastric pain, nausea, vomiting, severe diarrhea and hemorrhage. Due to its mutagenicity and carcinogenicity to human beings, it belongs to group 'A' human carcinogen (USDHHS 1991; Cieslak-Golonka 1996). In order to bring down the concentration of Cr(VI) to acceptable levels (WHO 2004), almost all the industries must have to treat their effluents before disposal (Ismail and Bedderi 2009; Ismail et al. 2013a, b). In order to potentially remove the toxic heavy metals from water streams, biosorption is an attractive alternate to traditional industrial effluent treatment processes as it utilizes the high surface area and electric charges present in biological materials which help to accumulate heavy metals (Fourest and Roux 1992; Ramya et al. 2015a). It is reported in the literature that the chemically modified natural adsorbents are much more advantageous in their efficiency than crude ones (Orr et al. 2004). Moreover, due to the capability of lowering heavy metal concentration to ppm level, wide range of availability and eco-friendly nature, the usage of biopolymers from agricultural wastes as adsorbents is attracting many industries (Deans and Dixon 1992). In continuation to the traditional adsorption isotherms (Ramya et al. 2015a, b, 2016), the present study was conducted during the year 2015 at Acharya Nagarjuna University, India, in which new isotherms (both two-parameter and three-parameter models) are employed to completely understand the mass transfer and surface interaction in the removal of chromium(VI) using three biosorbents (banana bunch-stem powder—BSP, sorghum stem powder—SSP and casuarinas fruit powder—CFP).

Materials and methods

Materials preparation and analytical methods

Acid treatment of the powdered raw agricultural waste materials, viz. banana bunch-stem (BSP), sorghum stem (SSP) and casuarinas fruit (CFP) of particle size 0.3–1.0 mm, was done using 1 N $\text{H}_2\text{SO}_4/\text{HNO}_3$ in order to improve the adsorption capacities as described in previous studies (Ramya et al. 2016). Advantage of acid treatment was manifested from the changes in surface area, pore volume and pore diameter of adsorbents which were determined with a Brunauer–Emmett–Teller

(BET) N_2 surface area analyzer (Nova 1000 version 3.70) (Table 1).

All the chemicals used are of analytical grade. The standard Cr(VI) stock solution was prepared by dissolving potassium dichromate in deionized water and diluted according to the required concentrations. The initial chromium(VI) concentration of the untreated sample was 20 mg L^{-1} .

Batch adsorption experiments were performed to study the chromium removal efficiency of each adsorbent with respect to parameters such as time (0–180 min), and initial Cr(VI) concentration ($10\text{--}70 \text{ mg L}^{-1}$) with common conditions such as 50 mL of chromium solution with initial concentration of 20 mg L^{-1} , 200 rpm, 30°C , 180 min contact time, 5 g L^{-1} adsorbent dose. After each experiment, chromium ion concentrations were measured by diphenyl carbazide method (ASTM 1972). Blank experiments were carried out to study the adsorption of chromium on the walls of batch reactor and were found to be negligible. Each experiment was repeated thrice, and average result has been reported. The relative errors in the experimental results were about 5%.

SEM, EDX and FT-IR studies

Scanning electron micrograph imaging of the biosorbent materials revealed rough surface with some pore formation before adsorption as an indication of large surface availability which helps for high adsorption (Ramya et al. 2015b) and a smooth surface covering of the pores after adsorption in all three cases of adsorbents. Further, EDX spectra of biosorbents (Wt% of chromium: before adsorption: BSP/SSP/CFP—0.00, after adsorption: BSP—0.24; SSP—0.15; CFP—0.16) supported the successful loading of Cr(VI) ions on the surface of sorbents.

From the study of FT-IR bands, adsorption of Cr(VI) ions can be partly attributed to electrostatic attraction due to the presence of functional groups such as acid, alcohol and amine [C–O, C=O and aliphatic C–H str in three biosorbents: 1026–1039, 1614–1689 and 2917–2920 cm^{-1} ; CFP: =C–H str, C=C str, phenolic group: above 3000, 1450–1550, 3737 cm^{-1} (s); SSP/BSP: –OH str of acid: 3305–3320 cm^{-1} (br)] (Ramya et al. 2015b).

Adsorption isotherm studies

In order to predict the overall adsorption performance of the biosorbents, Fowler–Guggenheim, Kiselev, Hill–de Boer, Frumkin, Sips, Jovanovic, Harkins–Jura, Halsey, Smith, El-Awady, Flory–Huggins and Redlich–Peterson isotherms are employed to the batch adsorption experimental data.

Table 1 Surface area, pore volume and pore diameter of adsorbents

Sample	Total surface area (m ²)	Specific surface area (m ² g ⁻¹)	Total pore volume (cc g ⁻¹)	Pore diameter (less than) (°A)	Average pore diameter (°A)
BSP (UT)	0.039	4.91	0.006	325.88	46.42
BSP (AT)	0.068	16.95	0.021	334.58	48.79
BSP (CA)	0.024	8.07	0.012	319.15	58.23
SSP (UT)	0.025	5.00	0.002	327.09	18.79
SSP (AT)	0.198	24.77	0.021	319.60	33.75
SSP (CA)	0.217	19.70	0.020	309.05	26.49
CFP (UT)	0.023	1.28	0.003	327.68	86.70
CFP (AT)	0.297	41.89	0.031	328.39	29.78
CFP (CA)	0.120	39.87	0.030	332.37	18.98

UT untreated, AT acid treated, CA after chromium adsorption

Adsorption diffusion study

The sorption of Cr(VI) ions onto BSP, SSP and CFP from their aqueous solutions may be considered as a liquid–solid phase reaction, and the diffusion of ions into the biosorbents is studied using liquid film diffusion, Dunwald–Wagner intra-particle diffusion and moving boundary models.

Results and discussion

Analysis of the equilibrium data using isotherm equations in an adsorption system is important to describe how adsorbate interacts with the biosorbent materials during the adsorption process. An adsorption isotherm is characterized by certain constants where values express the overall biosorption performance and affinity of the sorbent. This information also helps to find out the capacities of different sorbents and the optimization of the biosorption mechanism pathways, and effective design of the biosorption systems (Aytas et al. 2011). Several isotherm equations have been used for the equilibrium modeling of adsorption systems. In order to understand the interaction between adsorbate and adsorbate/adsorbent, the sorption data have been subjected to different two-parameter sorption isotherms, namely Fowler–Guggenheim, Frumkin, Hill–de Boer and Kiselev, and three-parameter Sips isotherm.

Fowler–Guggenheim isotherm

Fowler–Guggenheim equation in an ideal adsorption assumes the existence of lateral interactions among adsorbed molecules on a set of localized sites with weak interactions between molecules adsorbed on neighboring sites (Fowler and Guggenheim 1949; Koubaissy et al.

2012). This model explains that the random character of distribution of the sorbate molecules on the adsorbent surface is not significantly altered when the interaction energy among the adsorbed molecules is constant and independent of fractional coverage of the surface (θ) (Hamdaoui and Naffrechoux 2007). Equations (1) and (2) represent the Fowler–Guggenheim isotherm model.

$$\text{Nonlinear equation: } K_{\text{FG}}C_e = \frac{\theta}{1 - \theta} \exp\left(\frac{2\theta W}{RT}\right) \quad (1)$$

$$\text{Linear equation: } \ln\left[\frac{C_e(1 - \theta)}{\theta}\right] = -\ln K_{\text{FG}} + \frac{2W\theta}{RT}, \quad (2)$$

where K_{FG} is Fowler–Guggenheim equilibrium constant (L mg⁻¹) for adsorption of the adsorbate on an active site, which represents the interaction between the adsorbate and the adsorbent, C_e is the concentration at equilibrium adsorption, W is the empirical interaction energy between two molecules adsorbed on nearest neighboring sites (kJ mol⁻¹), R is ideal gas constant (8.314 J mol⁻¹ K⁻¹), T is thermodynamic temperature (K) and θ is the fractional coverage of the surface.

The slope of the Fowler–Guggenheim model graph ($\alpha = 2W\theta/RT$) gives information about the interaction between adsorbed molecules which can be predicted as repulsive when ' α ' is positive and as attractive when ' α ' is negative, whereas there is no interaction between adsorbed molecules when $\alpha = 0$ (Davoudinejad and Ghorbanian 2013). In other words, if the interaction between the adsorbed molecules is attractive ($W < 0$), the heat of adsorption will increase with loading which is due to the increased interaction between adsorbed molecules as the loading increases. However, if the interaction among adsorbed molecules is repulsive ($W > 0$), the heat of adsorption shows a decrease with loading. If there is no interaction between adsorbed molecules ($W = 0$), this Fowler–Guggenheim equation will reduce to the Langmuir



equation (Yonli et al. 2011). From Table 2 and Fig. 1a, the interaction energy (W) is negative, which envisages that there is an attraction between the adsorbed molecules indicating a possible interaction between the adsorbed molecules. Similar attraction between adsorbed molecules was reported earlier by Yonli et al. (2011) based on observed negative W values for the studied adsorbents.

Kiselev isotherm

This isotherm assumes the metal ion adsorption in localized monomolecular layer and the equation is expressed as Eqs. (3) and (4) (Kiselev 1958).

$$\text{Nonlinear form: } k_1 C_e = \frac{\theta}{(1 - \theta)(1 + k_n \theta)} \quad (3)$$

$$\text{Linear form: } \frac{1}{C_e(1 - \theta)} = \frac{k_1}{\theta} + k_1 k_n, \quad (4)$$

where ' θ ' is the surface coverage which is equal to q/q_s or $(1 - C_e/C_o)$, k_1 is Kiselev equilibrium constant ($L\ mg^{-1}$) and k_n is the constant of complex formation between adsorbed molecules/adsorbate and adsorbent. These parameters explain the plausible formation of complex between adsorbed molecules in the adsorption mechanism (Hamdaoui and Naffrechoux 2007). When $k_n > 0$, the adsorbed molecules form complex on adsorbent surface that improves adsorption. When $k_n \leq 0$, there will be no complex and for $k_n = 0$, the equation is similar to Langmuir equation (the straight line) (Davoudinejad and Ghorbanian 2013). In the present case, for adsorption of chromium(VI) metal ions on three adsorbents, k_n values are

found to be negative (Table 2) which indicates that there is no formation of complex between the adsorbed molecules. However, it is important to notice that the linearization is poor in terms of coefficient of determination (R^2) in all three cases of adsorbents. As the linearization is poor, any interpretation from Kiselev isotherm should be avoided in the present case. In addition, Kiselev equilibrium constants (k_1) are negative (Table 2, Fig. 1b), which is surprising because an equilibrium constant should be positive (Hamdaoui and Naffrechoux 2007). This reinforces the above proposal of avoiding the interpretation from Kiselev isotherm in the present case.

Hill-de Boer isotherm

Hill-de Boer model helps to verify the Fowler–Guggenheim isotherm assumptions by considering the lateral interaction among adsorbed molecules in a dynamic sorption system (Hill 1946; De Boer 1953). Hill-de Boer isotherm model equations are given in Eqs. (5) and (6).

$$\text{Nonlinear equation: } K_1 C_e = \frac{\theta}{1 - \theta} \exp\left(\frac{\theta}{1 - \theta} - \frac{k_2 \theta}{RT}\right) \quad (5)$$

$$\text{Linear equation: } \ln\left[\frac{C_e(1 - \theta)}{\theta}\right] - \frac{\theta}{1 - \theta} = -\ln K_1 - \frac{k_2 \theta}{RT}, \quad (6)$$

where K_1 is the Hill-de Boer constant ($L\ mg^{-1}$), θ is fractional coverage, R is universal gas constant ($J\ mol^{-1}\ K^{-1}$), T is temperature (K) and k_2 is the energetic

Table 2 Adsorption isotherm parameters for predicting adsorbate interactions for the sorption of Cr(VI) on to the surface of biosorbents BSP, SSP and CFP

Isotherm	Parameter	BSP	SSP	CFP
Fowler–Guggenheim	W ($kJ\ mol^{-1}$)	-18.100	-16.400	-17.747
	K_{FG} ($L\ mg^{-1}$)	1.13×10^{-5}	1.56×10^{-4}	1.50×10^{-5}
	R^2	0.966	0.936	0.953
Kiselev	k_1 ($L\ mg^{-1}$)	-5.074	-0.172	-2.670
	k_n	-1.671	-3.273	-1.743
	R^2	0.521	0.481	0.570
Hill-de Boer	K_1 ($L\ mg^{-1}$)	8.03×10^{-9}	9.85×10^{-5}	1.31×10^{-7}
	k_2 ($kJ\ mol^{-1}$)	72.677	40.105	61.971
	R^2	0.947	0.949	0.965
Frumkin	a_F	7.185	6.510	7.045
	$\ln K$	-11.390	-8.764	-11.110
	R^2	0.966	0.936	0.953
Sips	n	0.943	0.703	0.947
	$m = 1/n$	1.060	1.422	1.056
	K_s ($L\ mg^{-1}$)	0.180	0.030	0.566
	q_{max} ($mg\ g^{-1}$)	8.065	4.695	5.988
	R^2	0.996	0.997	0.993

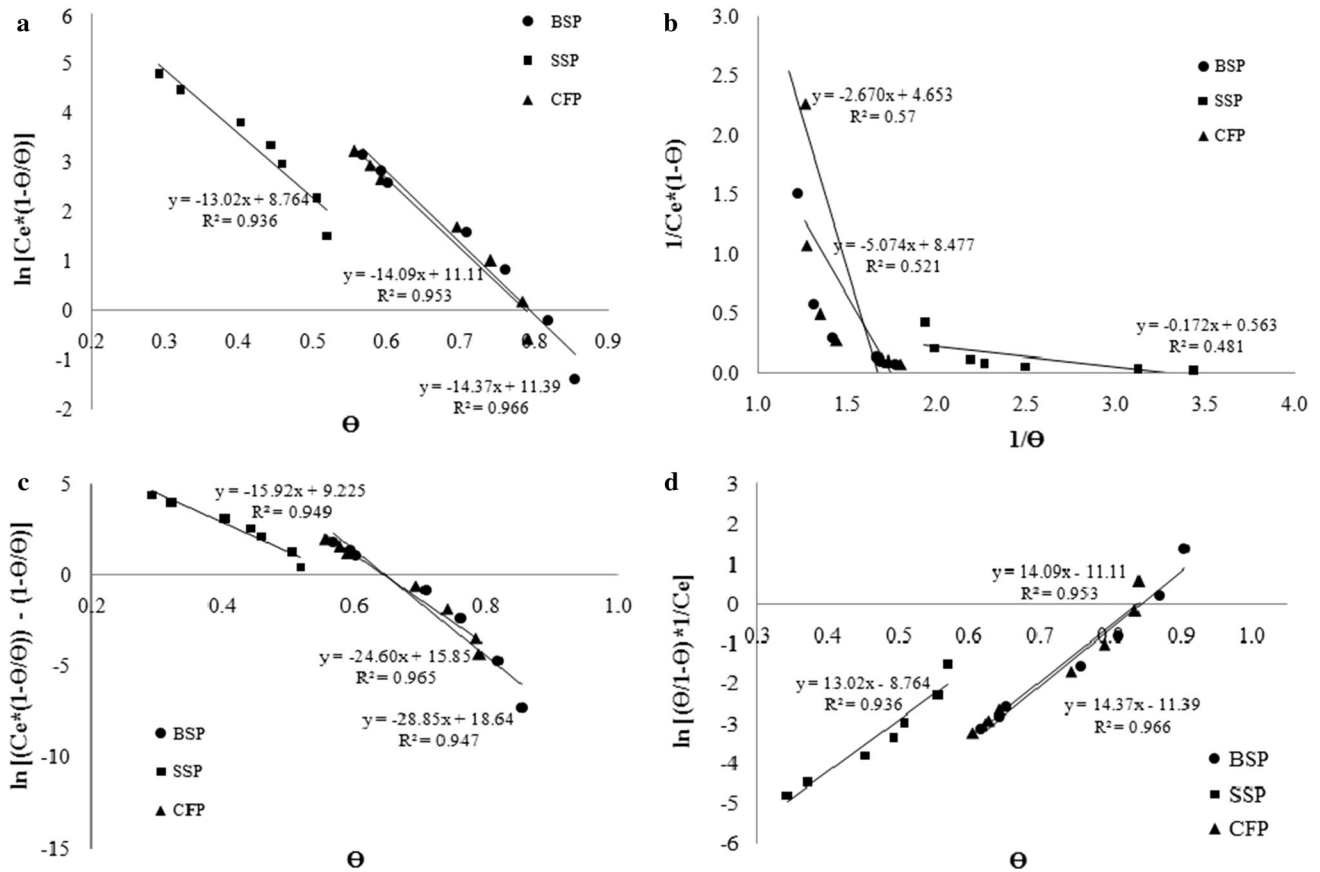


Fig. 1 a Fowler–Guggenheim, b Kiselev, c Hill–de Boer and d Frumkin adsorption isotherms for the removal of Cr(VI) using BSP, SSP and CFP

constant of the interaction between adsorbed molecules (kJ mol^{-1}).

From this isotherm, the interactions between adsorbed species are described as attractive, repulsive and no interaction when $k_2 > 0$, $k_2 < 0$ and $k_2 = 0$, respectively. Additionally, when $k_2 = 0$, this equation will reduce to the Volmer equation (Hamdaoui and Naffrechoux 2007). For the studied three adsorbents, the energetic constant of the interaction between adsorbed molecules (k_2) is positive (Fig. 1c, Table 2) which is an indication of attraction between the adsorbed molecules. This result is in agreement with the conclusion obtained using the Fowler–Guggenheim equation. Hence, formation of a multilayer can be predicted based on the possible attractions between adsorbed species.

Frumkin isotherm

Frumkin isotherm is another empirical interaction model which helps to elucidate the surface interactions of adsorbents in terms of Frumkin adsorption isotherm constant ‘ a_F ’. If the value of a_F is positive, then there is attractive interaction between the adsorbed species where as negative

‘ a_F ’ indicates repulsion (Vasudevan et al. 2010; Nwabanne and Okafor 2012). Nonlinear and linear forms of Frumkin isotherm are given as Eqs. (7) and (8), respectively.

Nonlinear equation: $\theta / (1 - \theta) e^{-2a_F \theta} = K C_e$ (7)

Linear equation: $\ln \left[\left(\frac{\theta}{1 - \theta} \right) \frac{1}{C_e} \right] = \ln K + 2a_F \theta$, (8)

where ‘ a_F ’ is the Frumkin interaction parameter between the adsorbate species and K is the Frumkin constant. The observed positive values of ‘ a_F ’ showed that attractive interactions are present between the adsorbed species (see Fig. 1d, Table 2), and hence, there is a possibility of multilayer formation which corroborates with the above two isotherms (Fowler–Guggenheim and Hill–de Boer).

Sips isotherm

Sips isotherm helps to circumvent the limitation of the rising adsorbate concentration associated with Freundlich isotherm model by combining it with Langmuir isotherm for predicting the heterogeneous adsorption systems (Sips

1948). Unlike the other adsorption isotherm models (Fowler–Guggenheim, Frumkin, Hill–de Boer and Kiselev), Sips model contains three parameters (q_{\max} , K_S and $1/n$), and the additional parameter—'n' values—is determined via trials and errors to obtain the maximum linear regression value of the isotherm graph (Fig. 2a). For single solute equilibrium data, the Sips model is expressed as Eqs. (9) and (10).

$$\text{Nonlinear SIPS isotherm equation: } q_e = \frac{q_{\max} K_S (C_e)^{1/n}}{1 + K_S C_e^{1/n}} \quad (9)$$

$$\text{Linear SIPS isotherm equation: } \frac{1}{q_e} = \frac{1}{q_{\max} K_S} \left(\frac{1}{C_e} \right)^{1/n} + \frac{1}{q_{\max}}, \quad (10)$$

where K_S is Sips isotherm model constant ($L\ g^{-1}$) and '1/n' (which is numerically equal to 'm') is the Sips isotherm model exponent. From the plot of '1/ q_e ' versus '(1/ C_e)^{1/n}', the values of K_S , q_{\max} and R^2 are obtained and are tabulated along with '1/n' (Table 2). When $m > 1$, a positive cooperativity between adsorbed molecules exists, whereas the contrary is considered for $m < 1$ (Cazalbou et al. 2015). From the results of Sips isotherm, positive cooperativity can be expected from 1/n values (Table 2) which are greater than unity in all three cases of adsorbents.

In order to determine the characteristic parameters for process design, mass transfer studies have been carried out using two-parameter isotherm models (Harkins–Jura, Halsey, Flory–Huggins, Smith and El-Awady) and three-parameter isotherm model (Redlich–Peterson).

Jovanovic isotherm

This model is similar to that of Langmuir model, except that the allowance is made in the former for the surface binding vibrations of an adsorbed species (Jovanović 1969; Arabloo et al. 2015). This model is given by using relationships Eqs. 11 and 12.

$$\text{Nonlinear form: } q_e = q_{\max}(1 - \exp(-K_J C_e)) \quad (11)$$

$$\text{Linear form: } \ln q_e = \ln q_{\max} - K_J C_e, \quad (12)$$

where K_J ($L\ g^{-1}$) is a Jovanovic parameter and q_{\max} ($mg\ g^{-1}$) is the maximum metal uptake. The estimated constants for the Jovanovic model are presented in Table 3. Poor correlation coefficient values indicate that monolayer adsorption is not only the sole mechanism in the removal of chromium(VI) using these three biosorbents (Fig. 3a).

Harkins–Jura isotherm

The Harkins–Jura adsorption isotherm considers the existence of heterogeneous pore distribution with multilayer formation. In other words, this model is merely based on the assumption of non-uniform adsorption sites distribution of the adsorbents and is not applicable unless a condensed film is shaped (Jura and Harkins 1946). This model is given by using Eqs. (13) and (14).

$$\text{Nonlinear form: } q_e = \sqrt{\frac{A_H}{B_H - \log C_e}} \quad (13)$$

$$\text{Linear form: } \frac{1}{q_e^2} = \frac{B_H}{A_H} - \frac{1}{A_H} \log C_e, \quad (14)$$

where A_H ($g^2\ L^{-1}$) and B_H ($mg^2\ L^{-1}$) are two parameters characterizing the sorption equilibrium. The values of

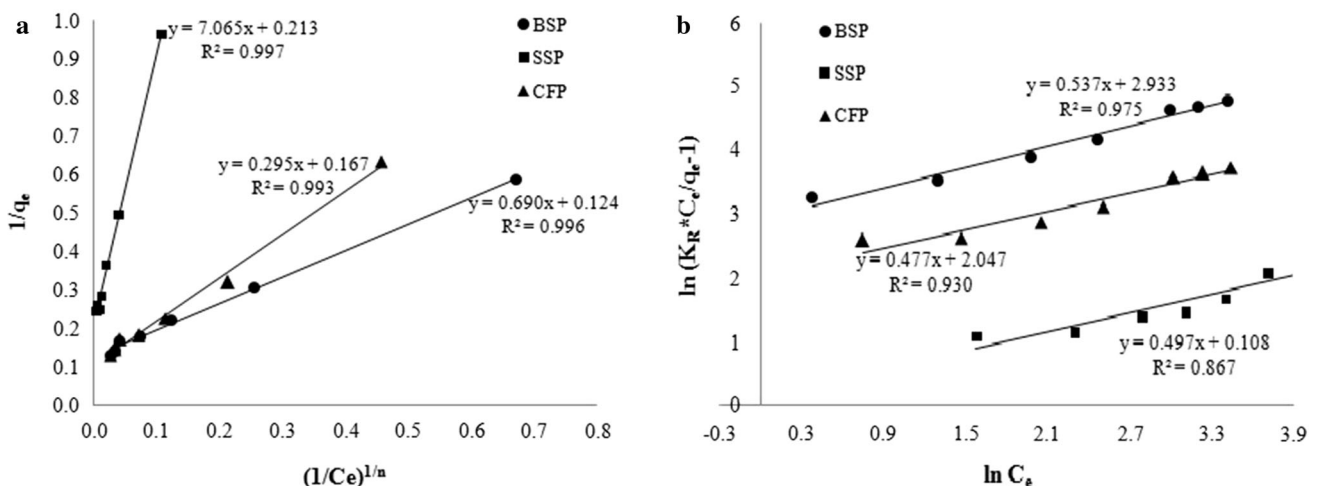


Fig. 2 Three-parameter isotherm models, viz. a Sips and b Redlich–Peterson for the removal of Cr(VI) using BSP, SSP and CFP

Table 3 Adsorption isotherm parameters for predicting mono-/multilayer adsorption of Cr(VI) on to the surface of biosorbents BSP, SSP and CFP

Isotherm	Parameter	BSP	SSP	CFP
Jovanovic	K_j (L g ⁻¹)	-0.042	-0.025	-0.043
	q_{max} (mg g ⁻¹)	2.588	1.478	2.399
	R^2	0.756	0.677	0.743
Harkins–Jura	A_H (g ² L ⁻¹)	4.739	1.314	3.717
	B_H (mg ² L ⁻¹)	1.365	1.586	1.364
	R^2	0.750	0.732	0.697
Halsey	n_{Ha}	-2.119	-1.704	-1.845
	K_{Ha} (mg L ⁻¹)	0.359	3.415	0.648
	R^2	0.967	0.920	0.948
Smith	$-W$	1.970	1.386	2.116
	W_b	27.950	18.070	29.320
	R^2	0.977	0.954	0.979
El-Awady	K_{ads}	0.019	0.116	0.018
	$1/y$	-1.898	-2.427	-2.188
	R^2	0.974	0.851	0.928
Flory–Huggins	n_{FH}	-0.381	-1.484	-0.466
	K_{FH} (L g ⁻¹)	0.085	0.036	0.078
	R^2	0.966	0.983	0.985
Redlich–Peterson	K_R (mg g ⁻¹)	31.750	0.850	10.760
	b_R	0.537	0.497	0.477
	a_R (mg L ⁻¹)	18.784	1.114	7.745
	R^2	0.975	0.867	0.930

coefficient of determination show that removal of chromium(VI) by these biosorbents does not obey Harkins–Jura adsorption isotherm (Fig. 3a, Table 3).

Halsey isotherm

Another multilayer supporting isotherm is the empirically derived Halsey isotherm which pertains only when the adsorption film thickens beyond two or three molecular layers of adsorbents, and the effect of the surface is largely smoothed out (Halsey 1948; Arabloo et al. 2015). This model equation is expressed as Eqs. (15) and (16).

$$\text{Nonlinear form: } q_e = \exp\left(\frac{\ln K_{Ha} - \ln C_e}{n_{Ha}}\right) \quad (15)$$

$$\text{Linear form: } \ln q_e = \frac{\ln K_{Ha}}{n_{Ha}} - \frac{\ln C_e}{n_{Ha}}, \quad (16)$$

where K_{Ha} (mg L⁻¹) and n_{Ha} are Halsey isotherm constants. For the Halsey adsorption isotherm, the best fitting of experimental data with reasonably good correlation coefficient values for chromium removal using BSP, SSP and CFP, respectively (Fig. 3b, Table 3) confirmed the

heteroporous nature of the adsorbents with multilayer formation.

Smith isotherm

The Smith model can be applied to multilayer and condensed water behaviors involved in the second region of the water sorption isotherm (Karaca et al. 2006). This isotherm considers the progressive enlargement of the adsorptive surface which accompanies swelling in an aqueous environment. The Smith isotherm equation is expressed by as Eq. (17).

$$\text{Smith equation: } q_e = W_b - W \ln(1 - a_w), \quad (17)$$

where a_w is water activity is during adsorption, q_e is the amount absorbed at equilibrium (mg g⁻¹), W and W_b are the constant parameters for the isotherm equation. Good regression values (R^2) of three adsorbents for the Cr(VI) removal using Smith isotherm (Fig. 3c, Table 3) further support the formation of multilayer of metal ions on the surface of the three biosorbents.

El-Awady isotherm

Unlike the Langmuir monolayer adsorption isotherm, El-Awady’s isotherm presumes multilayer adsorption or adsorption of single molecule on more than one active site (Gobara et al. 2015). Hence, the experimental data are fitted into the El-Awady model and the characteristic of the isotherm is given by Eq. (18).

$$\text{El-Awady equation: } \log \frac{\theta}{1 - \theta} = \log K - y \log C, \quad (18)$$

where θ is the degree of surface coverage, K_{ads} ($=K^{1/y}$) is the equilibrium constant of adsorption process and y represents the number of adsorbate molecules occupying a given active site. El-Awady isotherm gives information of the possibility of multilayer formation related to the ratio of $1/y$. If the ratio is less than unity, the formation of multilayers of adsorbed molecules on the surface is expected, whereas if the value of $1/y$ is greater than unity, it means that the adsorbed molecules plausibly occupy more than one active site (Obot et al. 2009). The literature survey shows that El-Awady’s isotherm is applied to understand the corrosion inhibition by adsorption of different organic molecules with high molecular weight (Gobara et al. 2015; Sabirneeza and Subhashini 2014; Karthikaiselvi and Subhashini 2014) and no report of application to metal ions adsorption is available. Also in the present study, the negative $1/y$ values (Table 3, Fig. 4a) for the El-Awady’s isotherm render suspicious the validity of this model for the Cr(VI) removal using all three biosorbents.

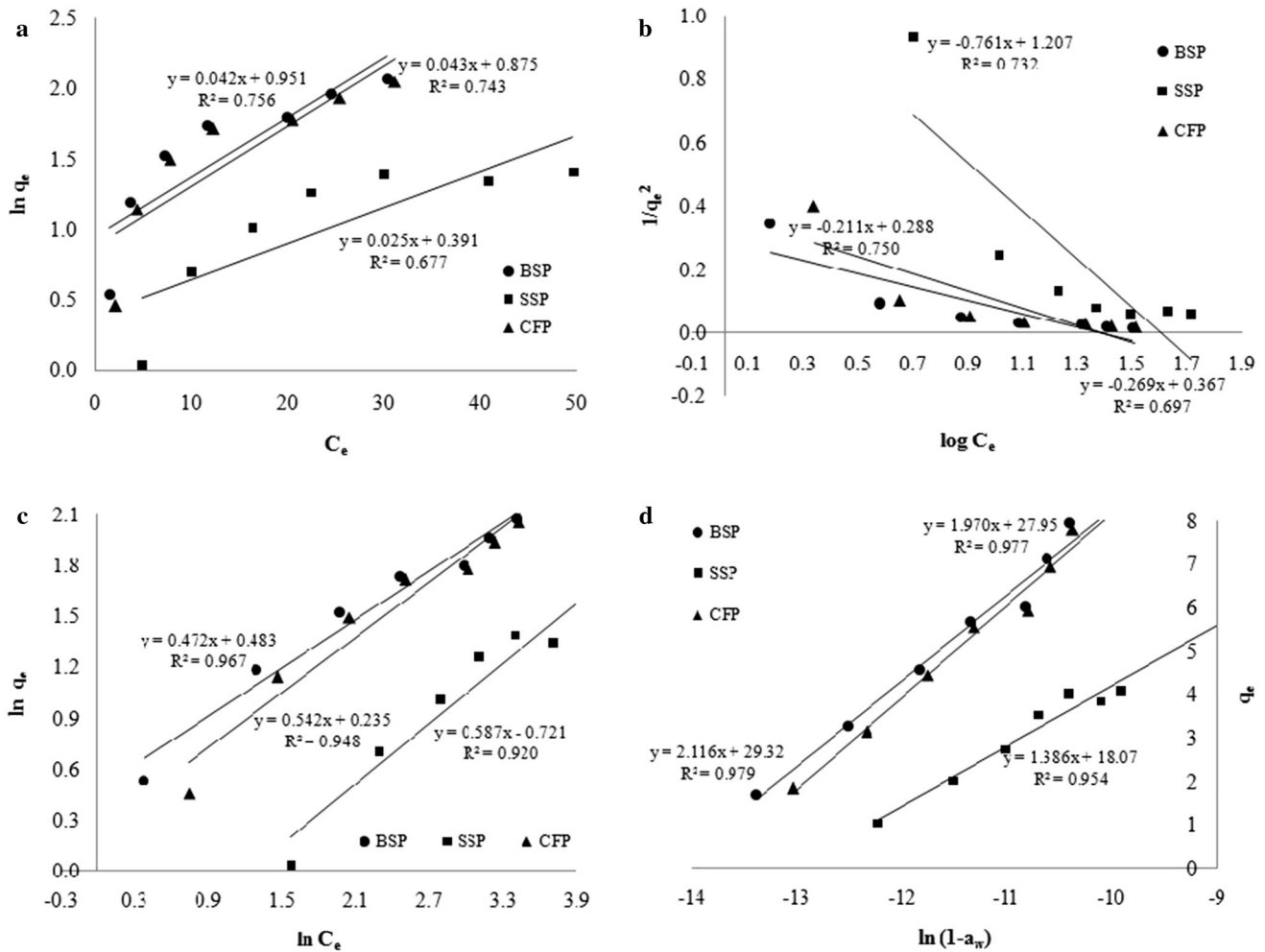


Fig. 3 a Jovanovic, b Harkins–Jura, c Halsey and d Smith adsorption isotherms for the removal of Cr(VI) using BSP, SSP and CFP

Flory–Huggins isotherm

The graph of Flory–Huggins isotherm equation drawn for $\log(1 - \theta)$ against $\log(\theta/C)$ gives a straight line with slope equal to n_{FH} and intercept is equal to $\log K_{FH}$ (Flory 1942; Huggins 1942). Nonlinear and linear forms of Flory–Huggins isotherm equation are expressed as Eqs. (19) and (20), respectively.

$$\text{Nonlinear form: } \frac{\theta}{C} = K_{FH}(1 - \theta)^{n_{FH}} \quad (19)$$

$$\text{Linear form: } \log \frac{\theta}{C} = \log K_{FH} + n_{FH} \log(1 - \theta), \quad (20)$$

where K_{FH} is Flory–Huggins equilibrium constant and n_{FH} is the numerical size parameter of metal ions occupying sorption sites.

If the value of the size parameter (n_{FH}) is greater than one, the formation of multilayer of adsorbate molecules on the surface of adsorbents can be predicted (Flory 1942; Huggins 1942). However, a value of n_{FH} less than unity

means that an adsorbate molecule will occupy more than one active site (Nwabanne and Okafor 2012). Similar to El-Awady isotherm model, in spite of good correlation values, negative n_{FH} values obtained from Flory–Huggins isotherm in all three cases of adsorbents (Table 3, Fig. 4b) show that Flory–Huggins isotherm is not applicable for removal of Cr(VI) ions by the present three biosorbents.

Redlich–Peterson isotherm

Redlich–Peterson isotherm incorporates the features of the Langmuir and Freundlich isotherms into a single equation, thereby facilitating the characterization of the adsorption equilibria over a wide concentration range (Prasad and Srivastava 2009). Nonlinear and linear RP isotherm equations can be expressed as Eqs. (21) and (22).

$$\text{Nonlinear RP isotherm equation: } q_e = \frac{K_R C_e}{1 + a_R C_e^{bR}} \quad (21)$$

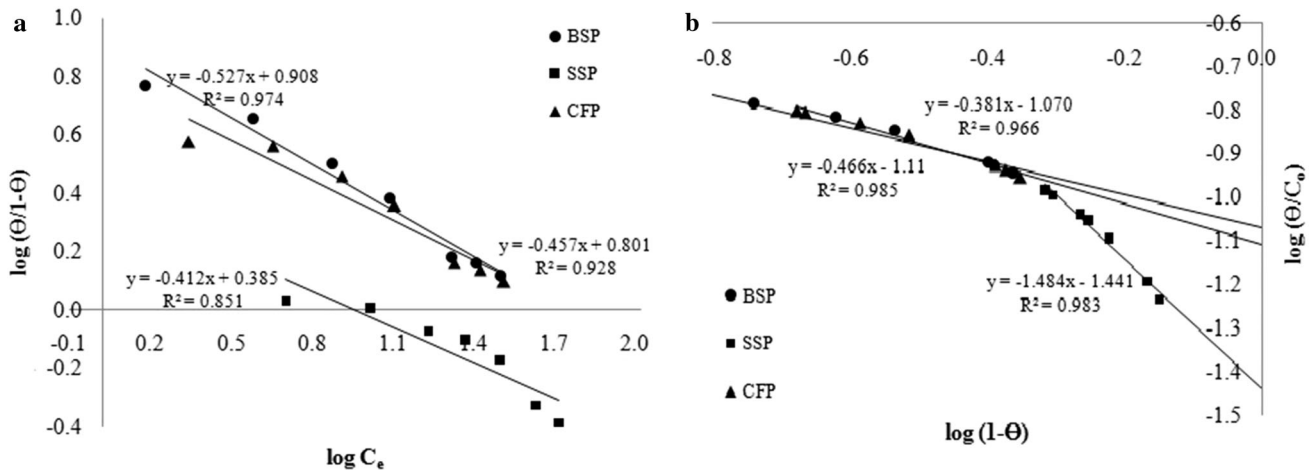


Fig. 4 **a** El-Awady and **b** Flory–Huggins isotherms for the removal of Cr(VI) using BSP, SSP and CFP

Linear RP isotherm equation: $\ln\left(K_R \frac{C_e}{q_e} - 1\right) = b_R \ln C_e + \ln a_R,$ (22)

where, K_R is the Redlich–Peterson adsorption capacity constant ($L g^{-1}$) which is determined via trials and errors in order to obtain the maximum linear regression value of the isotherm graph (See Fig. 2b), a_R is also a constant ($L mg^{-1}$) and b_R is an exponent ($0 < b_R < 1$). Since the exponent b_R lies between 0 and 1, it has two limiting behaviors: the Langmuir isotherm form for $b_R = 1$ and the Freundlich form for $b_R = 0$. However, the accuracy of these interpretations strongly depends on the fitting method (Kumara et al. 2014). From Table 3, it is clear that this model is in agreement with the experimental data and based on the b_R values for BSP, SSP and CFP lower than one and in the vicinity of 0.5, Redlich–Peterson adsorption isotherm studies describe the multilayer adsorptions in the present studied three biosorbents for the removal of Cr(VI) ions from aqueous system.

Hence, adsorption isotherm studies describe that both mono- and multilayer adsorptions occur in the cases of present studied three biosorbents in preference to the latter. Similar adsorption isotherm studies predicting the possibility of both mono- and multilayer adsorptions was reported earlier by other researchers (Li et al. 2015; Rathnakumar et al. 2009; Prapagdee et al. 2014).

Adsorption diffusion studies

In the adsorption system, the overall sorption rate can directly be affected by the mass transfer of solute or sorbate onto and within the sorbent particle. The rate at which the solute is removed from aqueous solution can be determined by studying the mass transfer mechanism which is useful to

apply the adsorption by solid particles to industrial uses. Hence, the overall adsorption process is assumed to occur using a three step model, viz. (1) diffusion of ions from the solution to the biosorbent surface, (2) diffusion of ions within the biosorbent and (3) chemical reaction between ions and the functional groups of biosorbent (Raji and Pakizeh 2014).

A quantitative study of the external mass transport of metal ions onto three biosorbents has been carried out, and results are discussed below.

The fractional attainment at equilibrium

The ratio of the amounts of sorbate removed from solution after a certain time to that removed when sorption equilibrium is attained gives the fractional attainment at equilibrium in which the rate of attainment of equilibrium is controlled either by film diffusion or by particle diffusion even though these two different mechanisms cannot be sharply demarcated (Imaga and Abia 2015). If the liquid film diffusion controls the exchange rate, Eq. (23) can be applied to the adsorption system.

$\ln(1 - F) = -k_{Fa}t,$ (23)

where $F(=q/q_e)$ —the fractional attainment of the equilibrium, k_{Fa} —the overall rate constant, t —time observed that the fractional attainment of equilibrium which can be calculated from the equation is an important parameter usually obtained from kinetic studies. D_r is the diffusion coefficient in biosorbent phase which can be calculated from Eq. (24) using values of k and r_0 (average radius of a biosorbent particle).

$k = -\frac{D_r \pi^2}{r_0^2}.$ (24)

Table 4 Diffusion study parameters for the adsorption of Cr(VI) ions on to the surface of biosorbents BSP, SSP and CFP

Adsorbent	Fractional attainment of equilibrium			Dunwald–Wagner			Moving boundary	
	k_{Fa} (min ⁻¹)	D_{Fa} (mm ² min ⁻¹)	R^2	k_{DW} (min ⁻¹)	D_{DW} (mm ² min ⁻¹)	R^2	k_{MB} (min ⁻¹)	R^2
BSP	0.029	1.18×10^{-4}	0.954	0.025	1.03×10^{-4}	0.932	0.005	0.969
SSP	0.020	0.81×10^{-4}	0.779	0.016	0.65×10^{-4}	0.779	0.004	0.790
CFP	0.017	0.69×10^{-4}	0.600	0.014	0.56×10^{-4}	0.623	0.003	0.553

For this model, the poor regression values (Table 4) show that the liquid film diffusion is not the sole controlling mechanism of exchange rate (Raji and Pakizeh 2014).

Dunwald–Wagner model

As mentioned earlier, the kinetic process of adsorption is always controlled by either liquid film diffusion or intra-particle diffusion; hence, one of these processes should be the rate limiting step (Imaga and Abia 2015; Abderrahim et al. 2011). In the case of diffusion of metal ions within the biosorbent, Dunwald–Wagner proposed an intra-particle diffusion model (Raji and Pakizeh 2014), which can be simplified into Eq. (25).

$$\log(1 - F^2) = -\frac{k_{DW}}{2.303}t. \quad (25)$$

Diffusivity coefficients in liquid film diffusion and intra-particle diffusion are almost equal in each case of adsorbent (Table 4). However, the order of diffusivity coefficients in liquid film diffusion/intra-particle diffusion is: BSP > SSP > CFP. Correlation data show that the diffusion models fits well for Cr(VI) sorption on BSP compared to SSP and CFP.

Moving boundary model

This model helps to describe the metal ions adsorption involving mass transfer accompanied by a chemical reaction with an assumption of a sharp boundary that separates a completely reacted shell from an unreacted core (Abderrahim et al. 2011). This boundary advances from the surface toward the center of the solid with the progression of adsorption. In this case, the rate is expressed as Eq. (26).

$$3 - 3(1 - F)^{2/3} - 2F = kt. \quad (26)$$

The correlation coefficient (R^2) values show that BSP is the only biosorbent that obey this model (Table 4).

Regeneration of the spent adsorbent and recovery of metal ions are highly enviable (Kumar et al. 2013) as the disposal of spent adsorbents is neither economical nor environmental friendly. Different methods (chemical, thermal, electrochemical, ultrasonic, solvent and

biological) for regeneration of spent adsorbents are well documented in the literature (Mishra 2014; Gautam et al. 2014; Kumar et al. 2007). Out of all the available methods, the prominent one is desorption with adequate eluents such as acids/alkalis/chelating agents (Lata et al. 2015). Hence, the present three biosorbents can be used on commercial scale for removal of chromium(VI) in view of possible regeneration of adsorbent, recovery of metal as well as based on the results of systematic study on surface interaction and mass transfer studies in the present case.

Conclusion

The use of abundantly available agricultural waste materials (banana bunch, sorghum stem and casuarinas fruit) as biosorbents for chromium(VI) removal from aqueous environment was investigated. High surface area and functional groups of adsorbents indicate the high possibility of Cr(VI) ions adsorption. Altogether adsorption isotherms describe that both mono- and multilayer adsorptions occur in the present studied three biosorbents in preference to the latter. From the diffusion study, the order of diffusivity coefficients in liquid film diffusion/intra-particle diffusion is BSP > SSP > CFP. Diffusion models fits well for Cr(VI) sorption to BSP compared to SSP and CFP. Hence, the efficient removal of Cr(VI) removal from wastewater could be achieved by utilizing these agricultural waste materials as adsorbents in large quantities.

Acknowledgements The authors are highly thankful to Acharya Nagarjuna University, SAIF (IIT-Madras), and Bangalore Institute of Technology for providing the support for conducting the research work and analysis of samples.

References

- Abderrahim O, Ferrah N, Didi MA, Villemin D (2011) A new sorbent for europium nitrate extraction: phosphonic acid grafted on polystyrene resin. *J Radioanal Nucl Chem* 290(2):267–275
- Arabloo M, Ghazanfari MH, Rashtchian D (2015) Spotlight on kinetic and equilibrium adsorption of a new surfactant onto sandstone minerals: a comparative study. *J Taiwan Inst Chem E* 50:12–23

- ASTM (1972) Annual book of ASTM standards part-23. American society for testing and materials, Philadelphia
- Aytas S, Turkozu DA, Gok C (2011) Biosorption of uranium (VI) by bi-functionalized low cost biocomposite adsorbent. *Desalination* 280(1):354–362
- Cattani E, Costa MJ, Torricella F, Levizzani V, Silva AM (2006) Influence of aerosol particles from biomass burning on cloud microphysical properties and radioactive forcing. *Atmos Res* 82(1):310–327
- Cazalbou S, Bertrand G, Drouet C (2015) Tetracycline-loaded biomimetic apatite: an adsorption study. *J Phys Chem B* 119(7):3014–3024
- Cieślak-Golonka M (1996) Toxic and mutagenic effects of chromium (VI) A review. *Polyhedron* 15(21):3667–3689
- Davoudinejad M, Ghorbanian SA (2013) Modeling of adsorption isotherm of benzoic compounds onto GAC and introducing three new isotherm models using new concept of Adsorption Effective Surface (AES). *Sci Res Essays* 8(46):2263–2275
- De Boer JH (1953) The dynamical character of adsorption. Oxford University Press, Oxford
- Deans JR, Dixon BG (1992) Uptake of Pb^{2+} and Cu^{2+} by novel biopolymers. *Water Res* 26(4):469–472
- Flory PJ (1942) Thermodynamics of high polymer solutions. *J Chem Phys* 10(1):51–61
- Fourest E, Roux JC (1992) Heavy metal biosorption by fungal mycelial by-products: mechanisms and influence of pH. *Appl Microbiol Biotechnol* 37(3):399–403
- Fowler RH, Guggenheim EA (1949) Statistical thermodynamics. Cambridge University Press, London, pp 431–450
- Gautam RK, Mudhoo A, Lofrano G et al (2014) Biomass-derived biosorbents for metal ions sequestration: adsorbent modification and activation methods and adsorbent regeneration. *J Environ Chem Eng* 2(1):239–259
- Gobara M, Baraka A, Zaghoul B (2015) Green corrosion inhibitor for carbon steel in sulfuric acid medium from “*Calotropis Gigantica*” latex. *Res Chem Intermed* 41(12):9885–9901
- Gustafsson Ö, Kruså M, Zencak Z et al (2009) Brown clouds over South Asia: biomass or fossil fuel combustion? *Science* 323(5913):495–498
- Guyon P, Frank GP, Welling M et al (2005) Airborne measurements of trace gas and aerosol particle emissions from biomass burning in Amazonia. *Atmos Chem Phys* 5(11):2989–3002
- Halsey G (1948) Physical adsorption on non-uniform surfaces. *J Chem Phys* 16(10):931–937
- Hamdaoui O, Naffrechoux E (2007) Modeling of adsorption isotherms of phenol and chlorophenols onto granular activated carbon: Part I. Two-parameter models and equations allowing determination of thermodynamic parameters. *J Hazard Mater* 147(1):381–394
- Hill TL (1946) Statistical mechanics of multimolecular adsorption II. Localized and mobile adsorption and absorption. *J Chem Phys* 14(7):441–453
- Huggins ML (1942) Some properties of solutions of long-chain compounds. *J Phys Chem* 46(1):151–158
- IARI (2012) Crop residues management with conservation agriculture: potential, constraints and policy needs. Indian Agricultural Research Institute, New Delhi
- Igwe JC, Abia AA (2003) Maize cob and husk as adsorbents for removal of Cd, Pb and Zn ions from wastewater. *Phys Sci* 2(8):83–94
- Imaga C, Abia AA (2015) Kinetics and mechanisms of chromium (VI) ion sorption using carbonized and modified sorghum (*Sorghum bicolor*) hull of two pore sizes (CMSH 150 μ m and 250 μ m). *Int J Chem Process Eng Res* 2(4):44–58
- Irwin A (2014) Black carbon: tackling crop-residue burning in South Asia. *Glob Change* 83:8–11
- Ismail Z, Bedderi AM (2009) Potential of water hyacinth as a removal agent for heavy metals from petroleum refinery effluents. *Water Air Soil Pollut* 199(1–4):57–65
- Ismail Z, Salim K, Othman SZ et al (2013a) Determining and comparing the levels of heavy metal concentrations in two selected urban river water. *Measurement* 46(10):4135–4144
- Ismail Z, Tai JC, Kong KK et al (2013b) Using data envelopment analysis in comparing the environmental performance and technical efficiency of selected companies in their global petroleum operations. *Measurement* 46(9):3401–3413
- Jovanović DS (1969) Physical adsorption of gases. I: isotherms for monolayer and multilayer adsorption. *Colloid Polym Sci* 235:1203–1214
- Jura G, Harkins WD (1946) Surfaces of solids. XIV. A unitary thermodynamic theory of the adsorption of vapors on solids and of insoluble films on liquid subphases. *J Am Chem Soc* 68(10):1941–1952
- Karaca S, Gürses A, Ejder M, Açıkyıldız M (2006) Adsorptive removal of phosphate from aqueous solutions using raw and calcinated dolomite. *J Hazard Mater* 128(2):273–279
- Karthikaiselvi R, Subhashini S (2014) Study of adsorption properties and inhibition of mild steel corrosion in hydrochloric acid media by water soluble composite poly (vinyl alcohol-*o*-methoxy aniline). *J Assoc Arab Univ Basic Appl Sci* 16:74–82
- Kiselev AV (1958) Vapor adsorption in the formation of adsorbate molecule complexes on the surface. *Kolloid Zhur* 20:338–348
- Koubaissy B, Toufaily J, El-Murr M et al (2012) Adsorption kinetics and equilibrium of phenol drifts on three zeolites. *Cent Eur J Eng* 2(3):435–444
- Kumar PA, Ray M, Chakraborty S (2007) Hexavalent chromium removal from wastewater using aniline formaldehyde condensate coated silica gel. *J Hazard Mater* 143(1):24–32
- Kumar KY, Muralidhara HB, Arthoba NY, Balasubramanyam J et al (2013) Low-cost synthesis of metal oxide nanoparticles and their application in adsorption of commercial dye and heavy metal ion in aqueous solution. *Powder Technol* 246:125–136
- Kumara NT, Hamdan N, Petra MI, Tennakoon KU, Ekanayake P (2014) Equilibrium isotherm studies of adsorption of pigments extracted from kuduk-kuduk (*Melastoma Malabathricum L.*) pulp onto TiO_2 nanoparticles. *J Chem*. doi:10.1155/2014/468975
- Lata S, Singh PK, Samadder SR (2015) Regeneration of adsorbents and recovery of heavy metals: a review. *Int J Environ Sci Technol* 12(4):1461–1478
- Li X, Li A, Long M, Tian X (2015) Equilibrium and kinetic studies of copper biosorption by dead *Ceriporia lacerata* biomass isolated from the litter of an invasive plant in China. *J Environ Health Sci Eng* 13(1):13–21
- Mishra SP (2014) Adsorption–desorption of heavy metal ions. *Curr Sci* 107(4):601–612
- Nwabanne JT, Okafor VN (2012) Adsorption and thermodynamics study of the inhibition of corrosion of mild steel in H_2SO_4 medium using *Vernonia amygdalina*. *JMMCE* 11(9):885
- Obot IB, Obi-Egbedi N, Umoren SA (2009) Adsorption characteristics and corrosion inhibitive properties of clotrimazole for aluminium corrosion in hydrochloric acid. *Int J Electrochem Sci* 4(6):863–877
- Orr PT, Jones GJ, Hamilton GR (2004) Removal of saxitoxins from drinking water by granular activated carbon, ozone and hydrogen peroxide: implications for compliance with the Australian drinking water guidelines. *Water Res* 38(20):4455–4461
- Prapagdee S, Piyatiratitvorakul S, Petsom A (2014) Activation of cassava stem biochar by physico-chemical method for stimulating chromium removal efficiency from aqueous solution. *Environ Asia* 7(2):60–69



- Prasad RK, Srivastava SN (2009) Sorption of distillery spent wash onto fly ash: kinetics and mass transfer studies. *Chem Eng J* 146(1):90–97
- Raji F, Pakizeh M (2014) Kinetic and thermodynamic studies of Hg(VI) adsorption onto MCM-41 modified by ZnCl₂. *Appl Surf Sci* 301:568–575
- Ramya PM, Jayasravanthi M, Venkata NR, Dulla BJ (2015a) Chemical oxygen demand reduction from coffee processing waste water: a comparative study on usage of biosorbents prepared from agricultural wastes. *GNEST J* 17(172):291–300
- Ramya PM, Jayasravanthi M, Venkata NR (2015b) Kinetic, thermodynamic and equilibrium studies on removal of hexavalent chromium from aqueous solutions using agro-waste biomaterials, *Casuarina equisetifolia L.* and *Sorghum bicolor*. *Korean J Chem Eng* 33(8):2374–2383. doi:10.1007/s11814-016-0078-6
- Ramya PM, Jayasravanthi M, Venkata NR (2016) Kinetic, isotherm and thermodynamics investigation on adsorption of divalent copper using agro-waste biomaterials, *Musa acuminata*, *Casuarina equisetifolia L.* and *Sorghum bicolor*. *Pol J Chem Technol* 18(2):1–10. doi:10.1515/pjct-2016-0031
- Rana P, Mohan N, Rajagopal C (2004) Electrochemical removal of chromium from wastewater by using carbon aerogel electrodes. *Water Res* 38(12):2811–2820
- Rathnakumar S, Sheeja RY, Murugesan T (2009) Removal of copper (VI) from aqueous solutions using teak (*Tectona grandis Lf*) leaves. *Int J Chem Mol Nucl Mater Metall Eng* 3(8):433–437
- Sabirneeza AA, Subhashini S (2014) Poly (vinyl alcohol–proline) as corrosion inhibitor for mild steel in 1 M hydrochloric acid. *Int J Ind Chem* 5(3–4):111–120
- Sharma AR, Kharol SK, Badarinath KV, Singh D (2010) Impact of agriculture crop residue burning on atmospheric aerosol loading: a study over Punjab State, India. *Ann Geophys Atmos Hydrosph* 28(2):367–379
- Sips R (1948) On the structure of a catalyst surface. *J Chem Phys* 16(5):490–495
- USDHHS, US Department of Health and Human Services (1991) Toxicological Profile for Chromium. Public Health Service Agency for Toxic substances and Diseases Registry, Washington, DC
- van der Werf GR, Randerson JT, Giglio L, Collatz GJ, Kasibhatla PS, Arellano AF Jr (2006) Inter-annual variability in global biomass burning emissions from 1997 to 2004. *Atmos Chem Phys* 6(11):3423–3441
- Vasudevan S, Lakshmi J, Sozhan G (2010) Studies relating to removal of arsenate by electrochemical coagulation: optimization, kinetics, coagulant characterization. *Sep Sci Technol* 45(9):1313–1325
- WHO, World Health Organization (2004) Guidelines for drinking-water quality, 3rd edn. Recommendations, Geneva
- Yonli AH, Khalid M, Batonneau-Gener I et al (2011) Removal of phenolic pollutants from water over BEA and HY zeolites in batch conditions. *J Chem Chem Eng* 5(5):429–434

